Human Molecular Genetics, 2013, Vol. 22, No. 3 **608–620**
doi:10.1093/hmg/dds470
Advance Access published on November 2, 2012

MicroRNA-205 regulates the expression of Parkinson's disease-related leucine-rich repeat kinase 2 protein

Hyun Jin Cho[1], Guoxiang Liu[1], Seok Min Jin[2], Loukia Parisiadou[1], Chengsong Xie[1], Jia Yu[1], Lixin Sun[1], Bo Ma[1], Jinhui Ding[3], Renée Vancraenenbroeck[4], Evy Lobbestael[5], Veerle Baekelandt[5], Jean-Marc Taymans[5], Ping He[6], Juan C. Troncoso[7], Yong Shen[6] and Huaibin Cai[1,*]

[1]Transgenics Section, Laboratory of Neurogenetics, National Institute on Aging, [2]Biochemistry Section, Surgical Neurology Branch, National Institute of Neurological Disorders and Stroke and [3]Computational Biology Core, Laboratory of Neurogenetics, National Institute on Aging, National Institutes of Health, Bethesda, MD 20892, USA, [4]Laboratory for biomolecular modeling and [5]Laboratory for Neurobiology and Gene Therapy, Katholieke Universiteit Leuven, Leuven B-3000, Belgium, [6]Roskamp Institute, Sarasota, FL 34243 and [7]Division of Neuropathology, Department of Pathology, The Johns Hopkins University School of Medicine, Baltimore, MD 21205, USA

Received July 24, 2012; Revised October 3, 2012; Accepted October 24, 2012

Recent genome-wide association studies indicate that a simple alteration of *Leucine-rich repeat kinase 2* (*LRRK2*) gene expression may contribute to the etiology of sporadic Parkinson's disease (PD). However, the expression and regulation of LRRK2 protein in the sporadic PD brains remain to be determined. Here, we found that the expression of LRRK2 protein was enhanced in the sporadic PD patients using the frontal cortex tissue from a set of 16 PD patients and 7 control samples. In contrast, no significant difference was detected in the level of *LRRK2* mRNA expression between the control and PD cases, suggesting a potential post-transcriptional modification of the LRRK2 protein expression in the sporadic PD brains. Indeed, it was identified that microRNA-205 (miR-205) suppressed the expression of LRRK2 protein through a conserved-binding site at the 3′-untranslated region (UTR) of *LRRK2* gene. Interestingly, miR-205 expression was significantly downregulated in the brains of patients with sporadic PD, showing the enhanced LRRK2 protein levels. Also, *in vitro* studies in the cell lines and primary neuron cultures further established the role of miR-205 in modulating the expression of LRRK2 protein. In addition, introduction of miR-205 prevented the neurite outgrowth defects in the neurons expressing a PD-related LRRK2 R1441G mutant. Together, these findings suggest that downregulation of miR-205 may contribute to the potential pathogenic elevation of LRRK2 protein in the brains of patients with sporadic PD, while overexpression of miR-205 may provide an applicable therapeutic strategy to suppress the abnormal upregulation of LRRK2 protein in PD.

INTRODUCTION

Parkinson's disease (PD) is a devastating neurodegenerative disorder, pathologically characterized by a preferential loss of dopaminergic (DA) neurons in the substantia nigra pars compacta (SNpc) and the presence of intracytoplasmic inclusions namely Lewy bodies and Lewy neurites in neurons (1). While the loss of DA neurons takes place in the SN, other brain regions, including the frontal cortex, develop Lewy bodies (2–5). An increasing number of genetic mutations have been identified as the genetic causes of PD (6), in which multiple missense mutations in the *Leucine-rich repeat kinase 2* (*LRRK2*) gene have been found to cause an autosomal-dominant form of familial PD (7,8). In addition to

*To whom correspondence should be addressed at: Transgenics Section, Laboratory of Neurogenetics, National Institute on Aging, National Institutes of Health, Building 35, Room 1A116, MSC 3707, 35 Convent Drive, Bethesda, MD 20892-3707, USA. Tel: +301 4028087; Fax: +301 4802830; Email: caih@mail.nih.gov

the familial mutations, recent genome-wide association studies (GWAS) reveal that the *LRRK2* gene locus is a genetic risk factor for the more common sporadic PD (9,10), indicating a potential alteration of *LRRK2* expression in the etiology of sporadic PD. In line with this notion, our previous studies in the PD mouse model demonstrate that overexpression of *LRRK2* accelerated α-synuclein-mediated neurodegeneration, while inhibition of LRRK2 expression ameliorated α-synuclein-induced neuropathology (11). These earlier genetic and transgenic studies raise the question of whether the level of LRRK2 protein expression is elevated in the brains of patients with sporadic PD, and then how the expression of LRRK2 protein is regulated.

MicroRNAs (miRNAs) are evolutionarily conserved small non-protein-coding transcripts that bind to partially complementary sites in the 3′-untranslated region (3′-UTR) of target messenger RNAs (mRNAs), and thereby control the translation of their target gene (12). A number of miRNAs have been associated with neuronal development, synaptic plasticity, memory formation and neurodegenerative diseases in the nervous system through regulating the translation of targeted genes (13,14). In particular, miR-133b has been indicated in the development of midbrain DA neurons (15). MiR-7 represses the expression of α-synuclein protein, and protects against α-synuclein-mediated cytotoxicity (16). Meanwhile, a recent report shows that LRRK2 is actively involved in the miRNA processing (17). However, there is no report on the miRNA modulating LRRK2 protein expression in PD brains.

Here, we examined the level of LRRK2 protein and *LRRK2*-targeting miRNAs in the frontal cerebral cortex of patients with sporadic PD. We found that the level of LRRK2 protein expression was significantly increased in the PD brains, whereas the level of miRNA-205 (miR-205) expression was decreased. We further demonstrated that miR-205 suppressed the expression of LRRK2 protein in the cell lines and primary neuron cultures through targeting its binding site in the 3′-UTR of *LRRK2* gene. Therefore, our findings suggest that miR-205 may serve as a potential biomarker in PD, and upregulation of the miR-205 level may provide a possible therapeutic avenue to inhibit LRRK2 expression in the sporadic PD.

RESULTS

The level of LRRK2 protein expression is increased in the frontal cortex of patients with sporadic PD

To investigate whether the steady-state expression of LRRK2 protein is altered in the brain of sporadic PD and sporadic PD with dementia (PDD) patients, we compared the expression level of LRRK2 protein in the frontal cortex of PD ($n = 8$) and PDD ($n = 8$) patients with age-matched non-pathological controls (NPCs, $n = 7$) (Fig. 1A and B). First, the specificity of the custom-made LRRK2 antibody (OC83A), recognizes both human and mouse LRRK2, was tested for western blot analyses (Supplementary Material, Fig. S1A–C). The densitometry of LRRK2 bands in the human brain samples was measured and normalized to β-actin for each sample (Fig. 1C). It was found that the expression of LRRK2 protein in the frontal cortex of PD and PDD patients was significantly upregulated compared with the NPC ($P < 0.05$, Fig. 1C). Moreover, the other LRRK2 antibody, provided by the Michael J. Fox Foundation (MJFF-2 (c41-2)), was used to detect increased LRRK2 protein levels in the frontal cortex of the PD patients to confirm this result (Supplementary Material, Fig. S1D and E). As a result, enhanced LRRK2 protein expression was observed in the brain of PD patients using two different LRRK2 antibodies. Meanwhile, the levels of *LRRK2* mRNA were comparable between NPC, PD and PDD cases (Fig. 1D). Also, to check whether increased LRRK2 protein levels in the RIPA-soluble fractions of PD brains are from altered detergent solubility, we extracted proteins from the RIPA-insoluble fraction using the 2% sodium dodecyl sulfate (SDS) buffer and LRRK2 proteins were detected by western blotting analysis using an MJFF-2 polyclonal LRRK2 antibody (Supplementary Material, Fig. S1F). As a result, we observed the LRRK2 proteins in the RIPA-insoluble fractions of human frontal cortex. In addition, the LRRK2 proteins in the RIPA-insoluble fraction showed

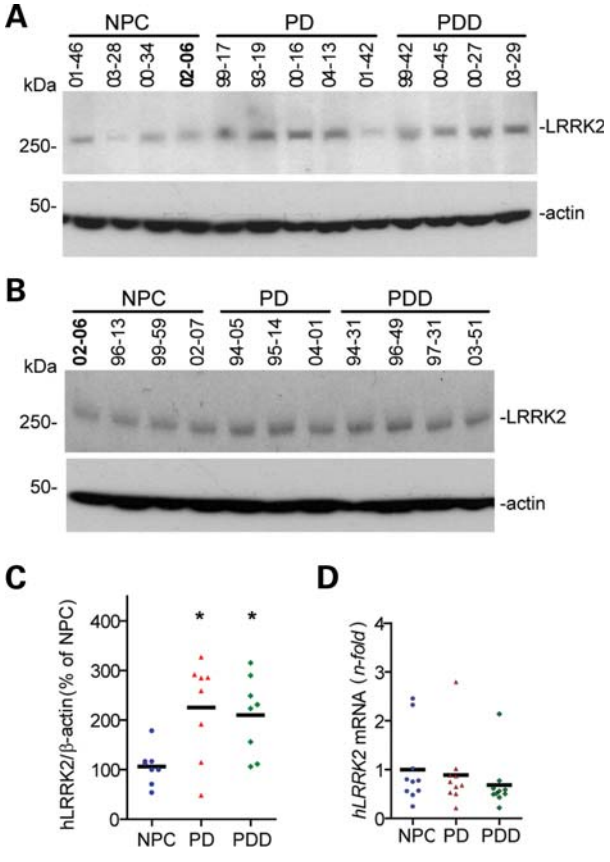

Figure 1. Level of LRRK2 protein is increased in the frontal cortex of sporadic PD patients. (**A**, **B**) Western blot analysis of LRRK2 protein expression (probed with OC83A antibody) in the frontal cerebral cortex of NPC, PD and PDD cases. The case number was shown on the top of each sample (Supplementary Material, Table S2). (**C**) LRRK2 protein levels for each sample were quantified. The LRRK2 bands of samples in the two different membranes were quantified using the 02-06 sample, loaded in both gels. NPC ($n = 7$), PD ($n = 8$) and PDD ($n = 8$) cases. $^{*}P < 0.05$ compared with NPC samples. (**D**) A scatter graph shows the expression of *LRRK2* mRNA in the frontal cerebral cortex of NPC, PD and PDD cases.

high levels in the PD brains compared with normal brains. This indicates that the differences in LRRK2 protein levels between NPC and PD cases do not reflect altered detergent solubility.

In addition to the frontal cortex, we also determined the levels of LRRK2 proteins in the striatal medium-sized spiny neurons and SNpc DA neurons of NPC and PD brain sections by immunohistochemistry using a commercial mouse monoclonal LRRK2 antibody (N138/6) that also recognizes both mouse and human LRRK2 proteins. The specificity of the N138/6 was tested using LRRK2 knockout brain extracts and sections (Supplementary Material, Fig. S2A and B). The striatal medium-sized spiny neurons were identified by co-staining with a marker protein CTIP2 (18). It was found that the intensity of LRRK2 immunoreactivity was significantly enhanced in the striatal neurons of PD cases compared with the NPC ($n = 18$ neurons for NPC and 19 neurons for PD; $n = 4$, 6 for NPC and PD cases; $P < 0.001$, Supplementary Material, Fig. S2C and D). Of note, the levels of *LRRK2* mRNA expression of the striatum were comparable between NPC and PD cases in quantitative real-time-PCR (qRT-PCR) analysis (Supplementary Material, Fig. S2E).

The levels of miR-205 are downregulated in the frontal cortex of sporadic PD patients

Considering that *LRRK2* mRNA levels showed no significant changes in the frontal cortex of the PD and PDD patients compared with the controls (Fig. 1D), the upregulation of LRRK2 protein expression in the frontal cortex region of patients with sporadic PD is unlikely caused by upregulated gene transcription. It was speculated that microRNAs could be responsible for the post-transcriptional regulation of LRRK2, as they suppress gene translation by binding to the specific regions within the 3′-UTR of the target gene in a sequence-dependent manner (19).

A number of putative miRNA target sites were identified in the 3′-UTR of both human and mouse *LRRK2* genes by silicon analysis using the TargetScan algorithm (20,21). We further narrowed down the conserved miRNAs across the different vertebrate species utilizing the UCSC whole-genome alignments program (http://genome.ucsc.edu). Of these, only the miR-205 targeting site, located at 103–123 bp downstream of the human *LRRK2* stop codon, is conserved among human, mouse, rat, dog and other vertebrates with a high score (Fig. 2A; Supplementary Material, Fig. S3).

Human miR-205 is located in chromosome 1q at position 1q32.2 and has been reported to show variable expression in a number of human carcinoma cell lines (22,23). To study the possibility that the expression of LRRK2 protein is regulated by miR-205, the levels of miR-205 were measured in the frontal cortex of NPC and PD cases by qRT-PCR (Fig. 2B). Interestingly, the frontal cerebral cortex of sporadic PD patients showed significantly lower levels of miR-205 expression than the controls ($n = 15$ for PD and $n = 11$ for NPC, $P = 0.0017$, Fig. 2B), whereas no significant difference was found between the patients with PD and PDD (Fig. 2B).

Moreover, statistically significant inverse correlation between the expression of LRRK2 protein and miR-205 was observed in the NPCs ($P = 0.0410$, $R^2 = 0.6029$, $n = 7$, Pearson's correlation), patients with PD ($P = 0.0166$, $R^2 = 0.6933$, $n = 7$) and patients with PDD ($P = 0.0250$, $R^2 = 0.6670$, $n = 7$) (Fig. 2C). When all of the samples were combined together, a more significant inverse correlation of LRRK2 protein and miR-205 expression was found ($P = 0.0001^{***}$, $R^2 = 0.5494$, $n = 21$; Fig. 2D).

To ensure the specificity of the decreased miR-205 level in PD patients, we also measured other highly scored putative miRNA expression levels in the frontal cortex of NPC, PD and PDD patients. The putative-binding sites for miR-181 and miR-19 are conserved among human, mouse, rat, dong and other vertebrates, although these two miRNA binding sites showed lower scores compared with the miR-205 binding site in the human *LRRK2* 3′-UTR (Table 1). Also, we checked other miRNA, miR-410, having a putative-responding site in the *LRRK2* 3′-UTR of the human brain samples. Interestingly, miR-181 (Fig. 2E), miR-19 (Fig. 2F) and miR-410 (Fig. 2G) revealed no significant differences between the normal and PD patient brains. Only the level of miR-205 expression was remarkably downregulated in the frontal cortex of PD patients compared with NPC.

In addition to the frontal cortex, miR-205 was significantly downregulated in the striatum of patients with sporadic PD compared with controls ($n = 4$ and 5 for NPC and PD cases, $P < 0.01$; Supplementary Material, Fig. S4A). And the levels of miR-410 expression showed no difference in NPC and PD cases (Supplementary Material, Fig. S4B). A similar inverse correlation was also observed in the striatum, although statistical significance could not be determined due to limited sample numbers ($P = 0.1679$, $R^2 = 0.3420$, $n = 7$; Supplementary Material, Fig. S4C). Together, these analyses support the hypothesis that the downregulation of miR-205 expression contributes, at least in part, to the elevation of LRRK2 protein expression in the brains of patients with sporadic PD.

Overexpression of miR-205 represses LRRK2 protein expression *in vitro*

To directly investigate the effect of miR-205 on LRRK2 protein expression, miR-205 precursor oligonucleotides (pre-miR-205) was transfected into the cells and the level of LRRK2 protein was analyzed by western blotting. Pre-miR is converted into mature miR by Dicer after it enters into the cells (24). It was observed that the treatment of HEK293T cells with pre-miR-205 consistently repressed LRRK2 protein expression by ~60% when compared with the cells treated with either vehicle (vcl) or a control scrambled pre-miRNA oligonucleotide ($P < 0.001$ versus control miRNA oligo, Fig. 3A). As a control, a similar reduction of the LRRK2 protein expression was detected in the cells treated with *LRRK2* small interference RNA (siRNA) ($P < 0.001$ versus control siRNA oligo, Fig. 3A). In addition, the efficacy of miR-205 in inhibiting the expression of LRRK2 protein was investigated in the primary cultured mouse cortical neurons. A similar reduction in the LRRK2 protein level was observed after treatment with pre-miR-205 ($P < 0.001$ versus control miRNA oligo, Fig. 3B). Also, in primary neuron cultures, there was a miR-205 dose-dependent reduction in LRRK2 protein levels of which 20 pmol of

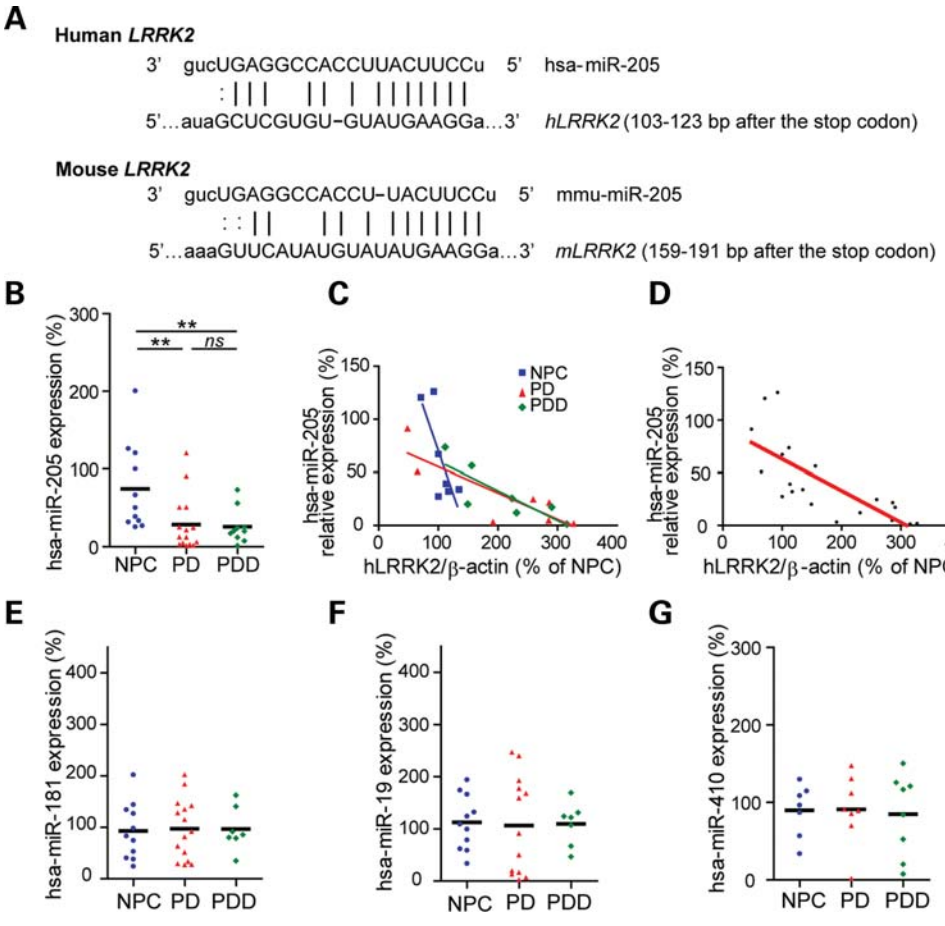

Figure 2. Increased levels of LRRK2 protein in the frontal cortex of the sporadic PD patients are correlated with the downregulation of miR-205. (**A**) The miR-205 target sites are located at 103–123 bp 3′-UTR of the human *LRRK2* stop codon and at 159–191 bp 3′-UTR of the mouse *LRRK2* stop codon. (**B**) Scatter plot shows hsa-miR-205 expression levels in the frontal cerebral cortex of NPC and PD/PDD cases. $^{**}P < 0.01$ compared with NPC samples; *ns* compared with PD samples. (**C**) Pearson's correlation test demonstrates a significant inverse correlation between hsa-miR-205 and LRRK2 protein expression in the frontal cortex of NPC ($P = 0.0410$, $R^2 = 0.6029$, $n = 7$), patients with PD ($P = 0.0166$, $R^2 = 0.7148$, $n = 7$) and patients with PDD ($P = 0.0250$, $R^2 = 0.6670$, $n = 7$). (**D**) Pearson's correlation test demonstrates a significant inverse correlation between hsa-miR-205 and LRRK2 protein expression in the frontal cortex of all human brain samples. (**E**–**G**) Scatter plots show miR-181 (E), miR-19 (F) and miR-410 (G) levels in the frontal cerebral cortex of NPC and PD/PDD cases.

pre-miR-205 resulted in 30% reduction of LRRK2 expression, while 40 pmol of pre-miR-205 reduced it by 50% (Fig. 3B). Next, to ensure whether the miR-205 affects the stabilities of LRRK2 protein and mRNA, we performed a pulse-chase experiment using cycloheximide to examine the degradation of LRRK2 protein and also carried out the qRT-PCR to measure the *LRRK2* mRNA in control oligo- or miR-205 oligo-transfected HEK293 cells. As a result, no significant alterations in the stabilities of LRRK2 protein and mRNA were observed between control oligo and miR-205-transfected cells (Supplementary Material, Fig. S5A and B).

We further examined the downregulation of LRRK2 protein at the cellular level using the HeLa cells transfected with a GFP-tagged pre-miR-205 expression vector (*GFP-miR-205*). Here, GFP was used to indicate the cells expressing exogenous miR-205. Consistent with the results from the western blot analysis, LRRK2 immunoreactivity was effectively downregulated by miR-205 in the GFP-positive cells (asterisks, Fig. 3Ca and Cb). In contrast, transfection of a control *GFP-CmiR* vector exhibits no effects on the signal intensity of LRRK2 protein (asterisk, Fig. 3Cc). Moreover, this miR-205-mediated suppression of LRRK2 also showed dose-dependent result. The signal intensity of LRRK2 immunostaining was reduced but still detectable in the cell having a low-GFP level (asterisk, Fig. 3Ca), whereas it was almost absent in the cell having a high-GFP level (asterisk, Fig. 3Cb).

A recent study also indicates that LRRK2 may interact with the miRNA processing pathway in regulating the protein synthesis (17). To investigate whether overexpression of wild-type or PD-related mutant LRRK2 affects the expression of miR-205, we measured the levels of miR-205 in the forebrain homogenates from 1-month-old non-transgenic (nTg), wild-type LRRK2 (wtLRRK2) overexpressing transgenic mice (CamKII-wtLRRK2) and LRRK2 G2019S mutant overexpressing transgenic mice (CamKII-G2019S) (11). As a result, it was identified that overexpression of either WT or G2019S LRRK2 did not significantly affect the levels of miR-205 expression in the mouse brains (Fig. 3D), indicating no regulation of miR-205 expression by enhanced LRRK2 protein levels.

Table 1. Conserved sites for miRNA families broadly conserved among vertebrates

	Predicted consequential pairing of the target region (top) and miRNA (bottom)	Context + score[a]
Position 116–123 of LRRK2 3′-UTR	5′ . . . AAAUAGCUCGUGUGUAUGAAGGA . . .	−0.36
	|||||||	
hsa-miR-205	3′ GUCUGAGGCCACCUUACUUCCU	
Position 505–511 of LRRK2 3′-UTR	5′ . . . AAAUAUUCAAAUGAAUUUGCACU . . .	−0.20
	|||||||	
hsa-miR-19b	3′ AGUCAAAACGUACCUAAACGUGU	
Position 505–511 of LRRK2 3′-UTR	5′ . . . AAAUAUUCAAAUGAAUUUGCACU . . .	−0.20
	|||||||	
hsa-miR-19a	3′ AGUCAAAACGUAUCUAAACGUGU	
Position 739–745 of LRRK2 3′-UTR	5′ . . . UUUCAACUCUAUGUUUGAAUGUG . . .	−0.04
	|||||||	
hsa-miR-181d	3′ UGGGUGGCUGUUGUUACUUACAA	
Position 739–745 of LRRK2 3′-UTR	5′ . . . UUUCAACUCUAUGUUUGAAUGUG . . .	−0.04
	|||||||	
hsa-miR-181a	3′ UGAGUGGCUGUCGCAACUUACAA	
Position 739–745 of LRRK2 3′-UTR	5′ . . . UUUCAACUCUAUGUUUGAAUGUG . . .	−0.04
	|||||||	
hsa-miR-181b	3′ UGGGUGGCUGUCGUUACUUACAA	
Position 739–745 of LRRK2 3′-UTR	5′ . . . UUUCAACUCUAUGUUUGAAUGUG . . .	−0.04
	|||||||	
hsa-miR-181c	3′ UGAGUGGCUGUCCAACUUACAA	

[a]The context + score for a specific site is the sum of the contribution of site-type, 3′-pairing, local AU, position, target site abundance and seed-pairing stability calculated as in Garcia *et al*. (38).

Next, to confirm the role of miR-205 in regulating the LRRK2 protein expression, the putative miR-205 targeting site of *LRRK2* was inserted at the 3′-UTR of a firefly luciferase reporter gene (p*GL3-LRRK2*). Then it was tested whether miR-205 affected the expression of the luciferase reporter in M17 cells. As a result, the luciferase activity of p*GL3-LRRK2* was significantly decreased by co-expression of miR-205, which was also dose-dependent ($P < 0.05$, 0.01 versus p*GL3-CXCR4* construct; Fig. 3E). In contrast, miR-205 showed no effect on the p*GL3-CXCR4* construct (negative control), which contains a chemokine receptor 4 siRNA binding site (Fig. 3E). Moreover, the co-expression of miR-205 with *pGL3* expression vector containing point mutations in the *LRRK2* miR-205 targeting site (*LRRK2-mUTR*) displayed no reduction in the luciferase activity (Fig. 3F). These results demonstrate that miR-205 suppresses the expression of LRRK2 protein through the direct targeting the 3′-UTR of *LRRK2*.

MiR-205 inhibitor enhances LRRK2 protein expression

Anti-miR miRNA inhibitors (miRNA inhibitors) are designed to specifically bind to the endogenous miRNAs and inhibit their activity on endogenous targets (25). Accordingly, it was identified that transfection of miR-205 inhibitors induced upregulation of LRRK2 protein expression in neuron cultures dose dependently. ($P < 0.05$ versus control oligo, Fig. 4A and B). In addition, neuron culture co-transfected with pre-miR-205 and miR-205 inhibitor exhibits no significant change in the levels of LRRK2 protein (Fig. 4A and B). Also, the luciferase activity of p*GL3-LRRK2* was significantly increased in the presence of the miR-205 inhibitor, whereas the negative control inhibitor and miR-29 inhibitor showed no effect on the luciferase activity ($P < 0.001$ versus control oligo; $P < 0.001$ versus control inhibitor; Fig. 4C). Together, these results demonstrate that endogenous miR-205 is a suppressor of LRRK2 protein expression in the cells.

MiR-205 treatment rescues the R1441G *LRRK2*-induced impairment of neurite outgrowth

LRRK2 is involved in the early development of neuronal processes (26). The neurons derived from transgenic mice overexpressing G2019S and Y1699C mutant forms of *LRRK2* display shortened neurites and reduced primary neurite numbers. To investigate whether miR-205 has the rescue effect on the impaired neurite outgrowth induced by mutant *LRRK2* expression, the miR-205 was introduced into the cultured hippocampal neurons derived from R1441G *LRRK2* transgenic mice (27). The bacterial artificial chromosome (BAC) clone used for generating the line of *LRRK2* transgenic mice containing 42 kb DNA fragment downstream of the stop codon of human *LRRK2*, and thereby it has the miR-205 binding site within the 3′-UTR of *LRRK2* gene. Similar to previous observations in neurons overexpressing G2019S or Y1699C *LRRK2*, the neurons expressing the R1441G *LRRK2* also displayed shortened neurites (Fig. 5Ab and B) and reduced neurite numbers (Fig. 5Ab and C) compared with littermate controls. Interestingly, the impaired neurite outgrowth was prevented by overexpression of miR-205 (Fig. 5Ad, B and C). However, overexpression of an irrelevant miRNA (miR-29) or a negative control miRNA (ngt ctrl) failed to rescue the neurite outgrowth defects in neurons from the *LRRK2* R1441G BAC transgenic mouse (Fig. 5A–C), indicating that this rescue result is the miR-205 specific effect.

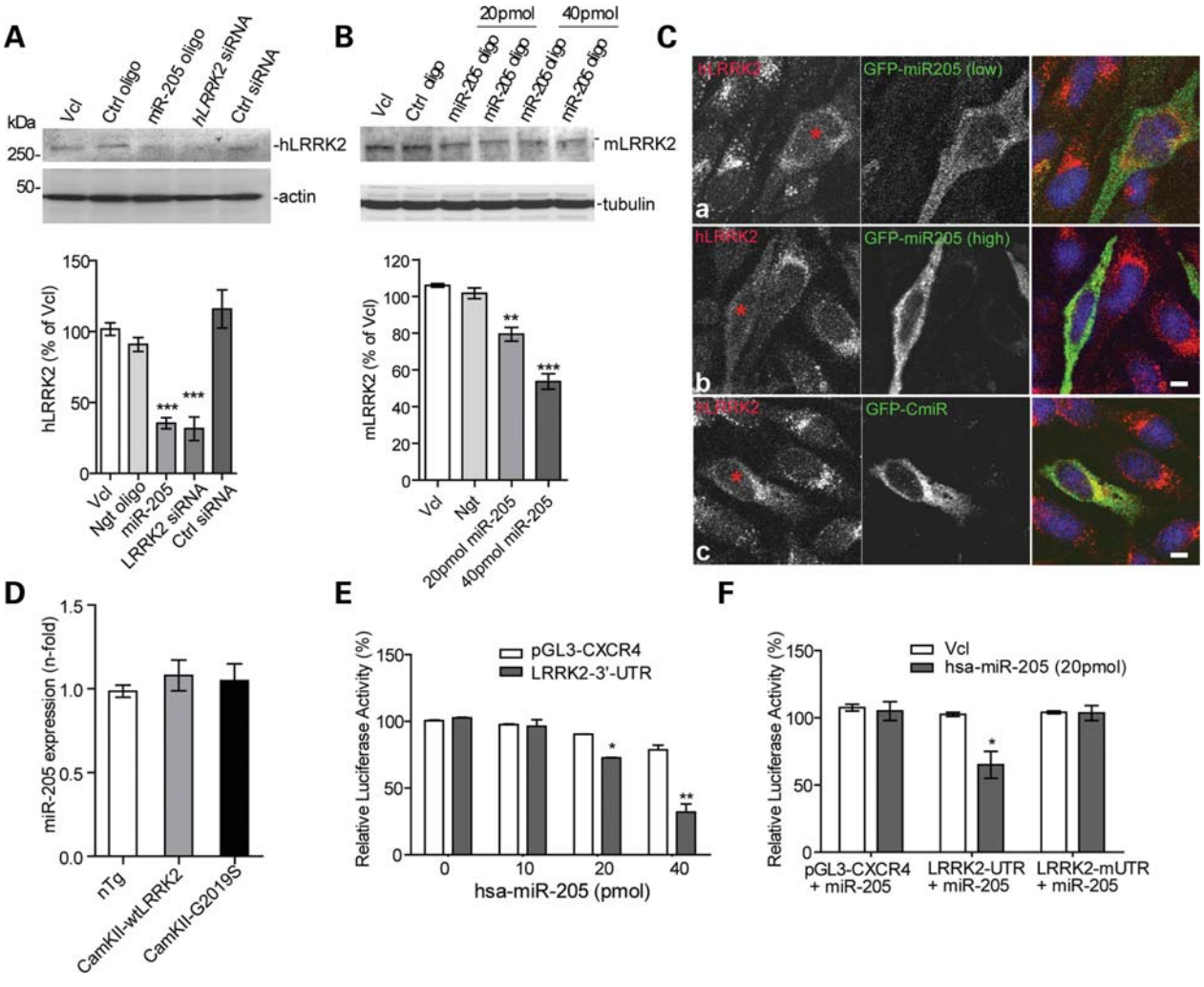

Figure 3. MiR-205 modulates LRRK2 protein expression *in vitro*. (**A**, **B**) Western blots show LRRK2 protein expression levels in pre-miR-205 oligo- or *LRRK2* siRNA-transfected HEK293T cells (A) and primary cultured mouse cortical neurons (B). A scrambled microRNA oligo (Ctrl oligo), a scrambled siRNA (Ctrl siRNA) and a vehicle (Vcl) only were used as negative controls. β-Actin or β-III tubulin was used as a loading control. Bar graphs depict the signal intensities of LRRK2-positive bands in the vehicle, microRNA and siRNA-treated samples. $^{**}P < 0.01$ and $^{***}P < 0.001$ compared with vehicle-treated cells. (**C**) Representative images show immunostaining of endogenous LRRK2 protein (red) in the HeLa cells transfected with low (a) or high (b) levels of GFP-miR205 (green) plasmids or control GFP-CmiR (c) plasmid. The transfected cells are marked by red asterisks. Scale bar: 20 μm. (**D**) Quantified miR-205 expression levels in the forebrain of 1-month-old CaMKII-wtLRRK2, CaMKII-G2019S and littermate nTg mice ($n = 3$ for each genotype). (**E**) Bar graph depicts the luciferase activities of the p*GL3-LRRK2* construct in the presence of increasing concentration of miR-205. Luciferase activity was normalized to the renilla luciferase activity. $^{*}P < 0.05$, $^{**}P < 0.01$ compared with 0 pmol miR-205-treated cells. (**F**) Luciferase activities of the *LRRK2*-mUTR in the presence of hsa-miR-205 (20 pmol). $^{*}P < 0.05$ compared with vehicle-treated cells.

Also, we checked the levels of LRRK2 mRNA and protein in cultured hippocampal neurons from the *LRRK2* R1441G BAC transgenic mouse after miR-205. As a result, the expression of *LRRK2* mRNA showed no significant changes in the miR-205-treated neurons compared with the control oligo- and miR-29 oligo-treated cells (Supplementary Material, Fig. S6A), while the expression of LRRK2 protein was significantly downregulated by treatment of miR-205 ($P < 0.01$ versus R1441G + ngt ctrl, Fig. 5D and E). These data indicate that transfected miR-205 efficiently downregulated LRRK2 protein expression in the cultured neurons derived from the *LRRK2* R1441G BAC transgenic mice and it showed no effects on the level of LRRK2 transcripts. Taken together, these results demonstrate that overexpression of miR-205 rescues the mutant *LRRK2*-induced neurite outgrowth defects through the suppression of LRRK2 protein expression.

Noticeably, miR-205-transfected *nTg* neurons showed a moderate increase in both the total neurite length and neurite numbers (Fig. 5Ac, B and C). However, these changes do not reach statistical significance, despite a significant reduction of LRRK2 protein expression was observed in these neurons (Fig. 5D and E). These observations in miR-205-treated *nTg* neurons are consistent with our previous findings in LRRK2 knockout neurons, in which only a moderate increase of neurite outgrowth was found in LRRK2-deficient neurons compared with control neurons (26).

Next, we tried to prove that the rescue effect of miR-205 on impaired neurite outgrowth in the R1441G *LRRK2*-expressing

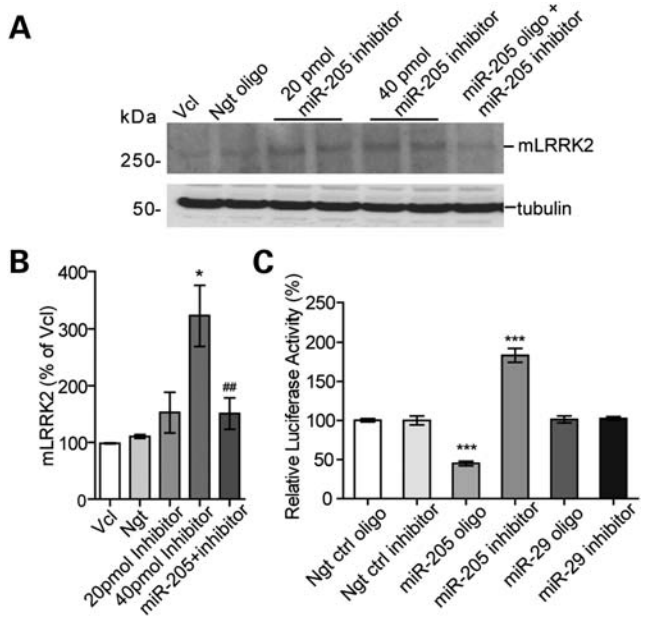

Figure 4. Treatment of miR-205 inhibitor upregulates LRRK2 protein expression. (**A**) Western blot shows a dose-dependent increase of endogenous LRRK2 protein expression in mouse primary cortical neurons treated with miR-205 inhibitor oligos. The total amount of oligos was the same for each treatment by adjusting with negative control oligos. (**B**) Bar graph shows the signal intensities of LRRK2-positive bands in vehicle (Vcl), miR-205 inhibitor oligo and miR-205 plus miR-205 inhibitor mixture oligo-treated samples. $^{*}P < 0.05$ compared with vehicle-treated cells. $^{\#\#}P < 0.01$ compared with 40 pmol inhibitor-treated cells. (**C**) Bar graph depicts the luciferase activity in the presence of 40 pmol of the miR-205 inhibitor, negative control (Ngt ctrl oligo), negative control inhibitor (Ngt ctrl inhibitor) and miR-29 inhibitor, respectively. The same amount of total oligos was applied to each condition. $^{***}P < 0.001$ compared with Ngt ctrl oligo-treated cells.

neurons is not the results produced by the indirect effect of miR-205. In the *LRRK2* G2019S transgenic mice (CaMKII-LRRK2 G2019S), the transgene contains only the coding region of *LRRK2* that lacks the miR-205 binding site (26). Using this mouse line, the same experiments were performed with control oligo, miR-205 and miR-29. As a result, it was observed that the treatment of miR-205 showed no rescue effect on the neurite outgrowth defects in the G2019S *LRRK2*-expressing neurons (Supplementary Material, Fig. S6B and C), indicating the specific rescue effect of the miR-205 on impaired neurite outgrowth in the *LRRK2* R1441G BAC transgenic mouse through targeting the 3′-UTR of LRRK2 gene.

To further investigate whether an miR-205 inhibitor exacerbates the neurite outgrowth defect induced by R1441G *LRRK2*, we transfected the negative control inhibitor (ngt ctrl inh), miR-205 inhibitor (miR-205 inh), and miR-29 inhibitor (miR-29 inh) into the neurons from *nTg* and *LRRK2* R1441G BAC transgenic mice. We found that R1441G *LRRK2*-expressing neurons treated with the miR-205 inhibitor showed shorter neuritis and reduced neurite numbers compared with the ngt ctrl inhibitor- and miR-29 inhibitor-treated R1441G *LRRK2* neurons (Fig. 5Fd, G and H). Interestingly, the miR-205 inhibitor revealed no effects on the *nTg* neurons (Fig. 5F–H), despite 2-fold increase in LRRK2 protein levels (Fig. 5I and J). These observations are consistent with our previous report that overexpression of wild-type *LRRK2* had no significant effects on the development of neuronal processes when compared with littermate controls (26). Taken together, the miR-205 inhibitor exacerbated the neurite outgrowth defect by upregulation of R1441G *LRRK2* protein expression.

Mouse midbrain DA neurons display a high level of miR-205 expression

To further establish the inverse correlation between LRRK2 protein and miR-205 expression *in vivo*, we checked the expression of LRRK2 protein and miR-205 in the cerebral cortex, hippocampus, midbrain, striatum and cerebellum of 1-month-old mice. As a result, the LRRK2 protein was highly expressed in the cerebral cortex, striatum and cerebellum; modestly expressed in the hippocampus; and barely detectable in the midbrain (Fig. 6A and B). Interestingly, the expression of *LRRK2* mRNA was comparable in the midbrain and hippocampus regions (Fig. 6C), suggesting a potential post-transcriptional regulation of LRRK2 protein expression in the midbrain. Consistent with this notion, we found the highest level of miR-205 expression in the midbrains of these mice (Fig. 6D). As a negative control, the level of miR-452 expression, putative miRNA for the 3′-UTR of mouse *LRRK2* but not conserved among the other species, was comparable in these brain regions (Fig. 6E). In addition, it was investigated whether the DA neurons are the main cells expressing miR-205 in the mouse midbrain region. To harvest the DA neurons, the laser capture microdissection (LCM) was performed and RNAs were extracted from isolated neurons for qRT-PCR analysis. We performed the qRT-PCR for the mRNA expressions of *GFAP*, *TH*, *Vmat2* and *DAT* genes in isolated DA neurons and astrocytes to confirm the genetic make-up of two cell populations (Supplementary Material, Fig. S7). As a result, the mRNA level of *GFAP*, the marker gene of astrocyte, was significantly high in the astrocytes compared with DA neurons (Supplementary Material, Fig. S7A). In contrast, the expression of the DA neuron markers such as *TH*, *Vmat2* and *DAT* was mainly observed in the nigral DA neurons but not in the astrocytes (Supplementary Material, Fig. S7B–D). Using these samples, it was found that the expression of miR-205 in midbrain DA neurons was extremely higher compared with the astrocytes (Fig. 6F), indicating that miR-205 is mainly expressed in the neurons of midbrain. Taken together, these results suggest that the high level of miR-205 expression may contribute to the low level of LRRK2 protein expression in the mouse midbrain region.

Because aging is a main factor contributing to the development of sporadic PD, we decided to study the aging-dependent changes of *LRRK2* protein, mRNA and miR-205 expression in the midbrain regions using 1-, 9- and 18-month-old mice. As a result, a significant reduction of LRRK2 protein was detected in an age-dependent manner (Fig. 6G and H). Next, it was investigated whether the alteration of LRRK2 protein expression in the older mice is correlated with the change in *LRRK2* mRNA levels. Consistent with previous results (28), there were no significant alterations of *LRRK2* mRNA levels in the midbrain between young and old mice (Fig. 6I). Finally, the levels of miR-205 expression in the midbrain of different

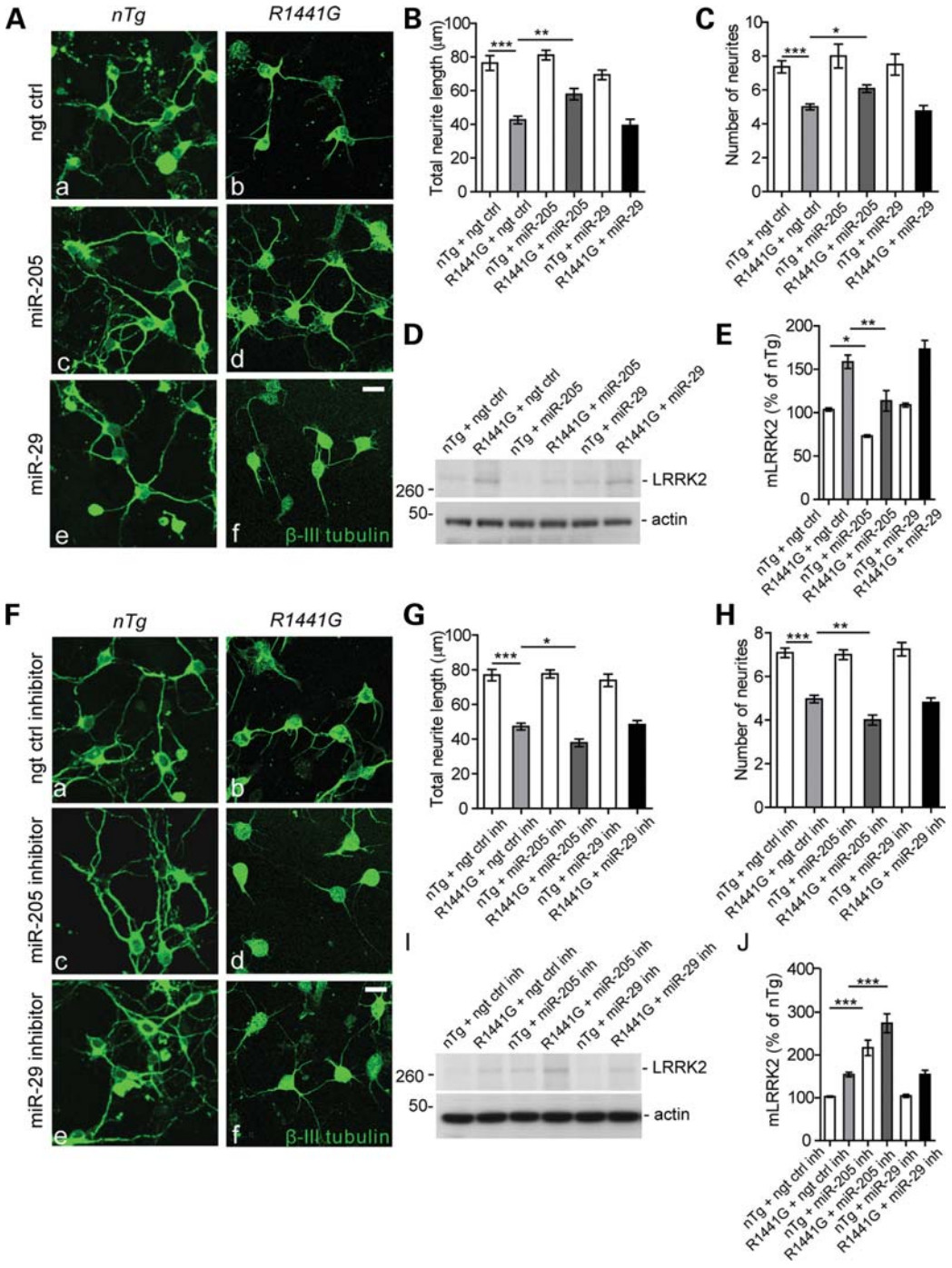

Figure 5. Pre-miR-205 precursor treatment rescues the neurite growth defects induced by R1441G *LRRK2*. (**A**) Representative images show cultured hippocampal neurons (2 DIV) derived from postnatal day 1 littermate non-transgenic (nTg, a, c, e) and R1441G *LRRK2* transgenic (R1441G, b, d, f) pups. The neurons were stained with β-III tubulin antibody (green) 24 h after transfection with a negative control (ngt ctrl) oligo (40 pmol; a, b), pre-miR-205 oligo (40 pmol; c, d) or pre-miR-29 oligo (40 pmol; e, f). Scale bar: 20 μm. (**B**, **C**) Bar graphs depict measurement of the total neurite length (B), and the number of primary neurites (C) from neurons under different treatment conditions. Fifty to 100 neurons were analyzed per genotype per condition. $^{*}P < 0.05$, $^{**}P < 0.01$ and $^{***}P < 0.001$. (**D**, **E**) Western blot shows alteration of LRRK2 protein expression in cultured hippocampal neurons from *nTg* and *LRRK2* R1441G pups. Three independent experiments were carried out for this study. $^{*}P < 0.05$, $^{**}P < 0.01$. (**F**) Representative images show cultured hippocampal neurons (2 DIV) derived from littermate non-transgenic (nTg, a, c, e) and R1441G *LRRK2* transgenic (R1441G, b, d, f) pups. The neurons were transfected with a negative control inhibitor (ngt ctrl inh) (40 pmol; a, b), miR-205 inhibitor (40 pmol; c, d) or miR-29 inhibitor (40 pmol; e, f). Scale bar: 20 μm. (**G**, **H**) Bar graphs show measurement of the total neurite length (G), and the number of primary neurites (H) from neurons under different treatment conditions. Fifty to 100 neurons were analyzed per genotype per condition. $^{*}P < 0.05$, $^{**}P < 0.01$, $^{***}P < 0.001$. (**I**, **J**) Western blot shows LRRK2 protein levels in cultured hippocampal neurons from *nTg* and *LRRK2* R1441G pups. Three independent experiments were carried out for this study. $^{***}P < 0.001$.

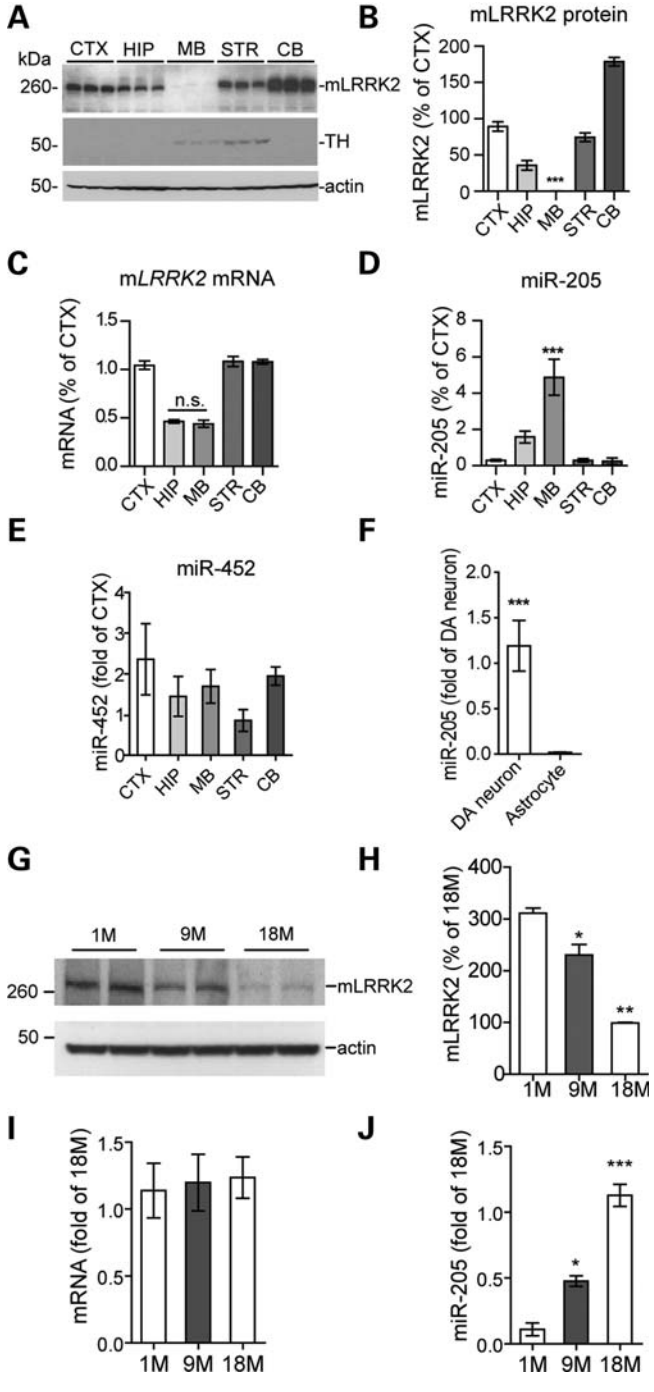

Figure 6. Regional distribution of LRRK2 protein and miR-205 expression in mouse brains. (**A**) Western blot of LRRK2 protein in different brain regions of 1-month-old mice. CTX, cerebral cortex; HIP, hippocampus; MB, midbrain; STR, striatum; CB, cerebellum. TH and β-actin were used as loading controls. (**B**–**E**) Bar graphs quantify the expression of LRRK2 protein (B), mRNA (C), miR-205 (D) and miR-452 as a negative control (E) in different brain regions. The relative expression is shown as a percentage of the mean using the cortex region as reference. $^{***}P < 0.001$. (**F**) Bar graph shows the quantification of miR-205 expression in the midbrain DA neurons and cultured primary astrocytes. In this experiment, U6 snRNA was used as a normalization control. $^{***}P < 0.001$. (**G**) Western blot analysis of LRRK2 protein expression in the midbrain of 1-, 9- and 18-month-old mice. (**H**–**J**) Bar graphs show quantification of LRRK2 protein (H), mRNA levels (I) and miR-205 levels (J) in the midbrain of 1-, 9-and 18-month-old mice. $^{*}P < 0.05$, $^{**}P < 0.01$ and $^{***}P < 0.001$.

age groups were measured using the qRT-PCR. Interestingly, it was found that the levels of miR-205 showed significantly higher expression in the midbrains of 18-month-old mice compared with the 1-month-old group ($P < 0.001$, Fig. 6J). Together, these data support an inverse correlation between the expression of LRRK2 protein and miR-205 in the mouse midbrain in the aging process. It suggests that the expression of LRRK2 protein can be dynamically regulated by miR-205 in the midbrain during the normal aging.

DISCUSSION

Missense mutations in *LRRK2* have been associated with both familial and sporadic forms of PD (29). Recent GWAS further raise the possibility that a simple alteration of *LRRK2* gene expression may contribute to the common sporadic PD (9,10). In support of this notion, here we showed that LRRK2 protein expression was significantly increased in the frontal cerebral cortex from patients with sporadic PD. Attempts have been made to examine the expression levels of LRRK2 protein in the brain of patients with familial and sporadic PD (30,31). However, it is difficult to draw conclusions from these early studies, because of the small sample sizes and the uncertainty of LRRK2 antibody's specificity. Here, we have characterized two LRRK2 antibodies that specifically recognized LRRK2 in the western blot and immunohistochemical analyses, in which *LRRK2* knockout tissues were used as negative controls. More critically, we were able to obtain a sufficient number of well-preserved frontal cerebral cortices of patients with sporadic PD/PDD and controls from the Sun Heath Institute (32) for LRRK2 protein expression study. Our western blot analysis demonstrated a significant increase of LRRK2 protein expression in the frontal cortex of patients with sporadic PD and PDD compared with the controls. In addition, it was detected that LRRK2 protein expression was also upregulated in the soma of striatal medium-sized spiny neurons of patients with sporadic PD by immunostaining of paraffin-embedded SNpc sections. Also, we tried to investigate the LRRK2 protein levels in the SNpc region of PD patients. Because of huge cell loss in this brain region, immunohistochemistry analysis was performed to observe anti-LRRK2 immuno-intensity in each DA neuron instead of western blot analysis. Consistent with the notion of very low *LRRK2* expression in the SNpc DA neurons (28,33), no apparent LRRK2-positive staining was observed in the neuronal cell body of either NPC or PD cases (Supplementary Material, Fig. S8A). Instead, more LRRK2-positive puncta were found along the processes of DA neurons in the PD cases compared with the controls (Supplementary Material, Fig. S8A and B).

Also, we further examined the cell-type distribution of LRRK2 in the brain of 1-month-old mice by immunohistochemistry using an LRRK2 N138/6 antibody. LRRK2 protein was more enriched in the soma of neurons compared with the astrocytes and microglia (Supplementary Material, Fig. S8C). The neurons, astrocytes and microglia were identified by co-staining with the respective marker proteins: neuronal nuclei (NeuN), glial fibrillary acidic protein (GFAP) and ionized calcium-binding adaptor molecule 1 (IBa1). This

indicates that LRRK2 protein expression may be more contributed by neurons in the brains of NPC and PD cases.

By silicon analysis of the 3′-UTR of human *LRRK2* gene and its vertebrate orthologs, we identified a conserved miR-205-binding site across different vertebrate species. Previous studies demonstrate that miR-205 modulates the expression of low-density lipoprotein receptor-related protein 1, a multifunctional endocytic receptor that plays essential roles in the pathogenesis of Alzheimer's disease (34). In addition, miR-205 has been shown to be overexpressed in some types of tumors such as head and neck squamous cell carcinoma while it is significantly downregulated in the breast tumors compared with the matched normal tissue (22,23). These reports indicate that miR-205 may involve a variety of important biological and pathological pathways. We examined the levels of miR-205 in the frontal cerebral cortex and striatum of patients with sporadic PD and controls. We found an inverse correlation between LRRK2 protein and miR-205 expression in the brains of PD and control cases. To study the levels of LRRK2 protein and miR-205, we performed main experiments using the frontal cortex, a brain region that has the projection of DA neurons. Although the frontal cortex of PD patients shows no pronounced cell death like the SNpc region, it is still molecularly and pathologically affected in PD brains (2–5) and shows the biochemical alterations involved in the disease process. While the SNpc region of sporadic PD is almost completely depleted of DA neurons by the time of autopsy, the frontal cortex shows no dramatic neuronal cell death. Nevertheless, the frontal cortex has the Lewy bodies during the disease. So the study with the frontal cortex of sporadic PD patients can reveal pathogenically relevant disease changes.

Next, we identified the same inverse correlation of LRRK2 protein and miR-205 expression in the mouse brain diverse regions, especially in the midbrain, in which the highest level of miR-205 expression but the lowest level of LRRK2 protein expression was observed. The expression of LRRK2 protein and miR-205 was also dynamically regulated and inversely correlated in this region between young and old mice, suggesting a potential post-transcriptional regulatory role of miR-205 in modulating the LRRK2 protein expression during aging. These findings may also suggest that the maintenance of a low level of LRRK2 expression by miR-205 is important for the function and survival of midbrain DA neurons.

Indeed, we observed that overexpression of miR-205 suppressed the expression of LRRK2 protein in both cell lines and primary neuronal cultures, and prevented the neurite outgrowth defects induced by PD-related *LRRK2* R1441G expression.

However, it remains unclear how miR-205 expression is downregulated in the brains of patients with PD. A recent report indicates an involvement of DNA methylation in modulating the expression of miR205 in cancer cells (35). Further studies on DNA methylation or other modifications of the miR-205 gene locus in the brains of patients with PD may provide the mechanistic insights into the alteration of miR-205 expression in patients with sporadic PD.

In summary, here we provide evidences of increased LRRK2 protein expression in the PD brains as a potential causative factor in the pathogenesis of sporadic PD. We further reveal a novel regulatory mechanism of LRRK2 protein expression through miR-205, and suggest that miR-205 may serve as an applicable biomarker and a therapeutic target in the sporadic PD.

MATERIALS AND METHODS

Human brain tissues

Rapidly autopsied frontal cerebral cortices (within 3 h of the postmortem interval) were obtained from the Brain and Body Donation Program of the Banner Sun Health Research Institute (32). Striatal tissues and paraffin-embedded striatum as well as SNpc sections were obtained from the brain bank of Johns Hopkins University School of Medicine. Subjects or their legal representatives signed informed consents approved by the Banner Health and Johns Hopkins Institutional Review Boards. The diagnosis of PD was made based on the clinicopathological criteria including characteristic clinical features and on the presence of Lewy bodies within the pigmented neurons lost in the substantia nigra. Subjects with PD were divided into two groups on the basis of the presence or absence of clinically documented dementia. NPCs were selected based on the absence of cognitive impairment, Parkinsonism and Lewy bodies. Tissues of patients with autosomal recessive juvenile Parkinsonism, a relatively rare syndrome that shares many features of Parkinsonism, but without the presence of Lewy bodies or Lewy neurites, were excluded from this study. The average age at death for the PD subjects included in this study was 80 ± 6.9 years old, while for the NPC subjects it was 85 ± 6.6 years old (Supplementary Material, Tables S1 and S2).

Western blot analysis

Protein extracts for western blots were prepared as described previously (26). Briefly, brain tissue or isolated cells were sonicated in RIPA buffer (Sigma, St Louis, MO, USA) in the presence of protease inhibitor cocktail, PMSF, and phosphatase inhibitor cocktails 1 and 2 (all from Sigma). Lysates were then centrifuged at 4°C for 15 min at 14 000 rpm to get the supernatant of particulate and insoluble matter. For the RIPA-insoluble fraction, SDS lysis buffer (2% SDS, 10 mM EDTA, 50 mM Tris, pH 8.0 and PMSF) was added to the pellet and then sonicated. Protein concentration was determined using the bicinchoninic acid (BCA) assay kit (Pierce, Rockford, IL, USA). For western blotting, 20 μg of protein was separated by polyacrylamide gel electrophoresis using NuPage 4–12% Bis-Tris gels (Invitrogen, Carlsbad, CA, USA) in NuPAGE MOPS SDS Running buffer (Invitrogen). To ensure efficient transfer of proteins, gels were incubated in 2 × NuPAGE transfer buffer with methanol at room temperature for 20 min. The separated proteins were then transferred to nitrocellulose using the iBlot Dry Blotting system (Invitrogen) for 7 min and incubated with specific primary antibodies.

Antibodies

The polyclonal LRRK2 antibody (OC83A) was generated by immunization of rabbits with a histidine-tagged recombinant peptide corresponding to the residues 982–1280 of human LRRK2. The monoclonal LRRK2 antibody (N138/6) was obtained from UC Davis/NIH Neuromab Facility (Davis, CA, USA). Polyclonal antibodies (4EC9E and 4C84E) against murine LRRK2 were described previously (26). The other antibodies used for immunohistochemistry were glial fibrillary acidic protein (GFAP) (Sigma-Aldrich USA, St Louis, MO, USA), ionized calcium-binding adaptor molecule-1 (Iba1) (Wako Chemicals USA, Richmond, VA, USA), tryosine hydroxylase (TH) (Pel-Freez Biologicals, Rogers, AR, USA) and HA (1:500, Santa Cruz Biotech, Santa Cruz, CA, USA). Monoclonal β-actin and β-III tubulin antibodies (all from Sigma) were used as loading controls or to visualize neurites, respectively.

Quantitative real time PCR

Total RNAs were prepared from brain tissues using the Mercury RNA isolation kit (Exiqon, Vedbaek, Denmark) according to the manufacturer's protocol. For *LRRK2* mRNA, reverse transcription was performed using the RT^2 First Strand kit (SABiosciences, Fredrick, MD, USA) and a real-time PCR was performed using the Taqman PCR mix (Applied Biosystems, Foster City, CA, USA) in the ABI's 7900HT Fast Real-Time PCR system (Applied Biosystems). The levels of *LRRK2* mRNA expression were normalized to *actin* mRNA. The primers for human or mouse *LRRK2* were: 5′-AGCAGGACAAAGCCAGCCTCA-3′ and 5′-GAT GGCAGCATTGGGATACAG-3′. The primers for mouse β-actin were: 5′-CGTTGACATCCGTAAAGACC-3′ and 5′-GCTAGGAGCCAGAGCAGTAA-3′. The primers for the human β-actin were purchased from SABiosciences. For qRT-PCR of miRNA, a miRCURY LNA first-strand cDNA kit (Exiqon) was used for the reverse transcription reaction, and qRT-PCR was performed using miRCURY LNA miR-205, miR-410, miR-452 and miRCURY LNA SYBR Green master mix (Exiqon) according to the supplier's instruction. U6 snRNA was used as a normalization control (Exiqon) for both human and mouse samples. The primers for the miR-181 and miR-19 were purchased from Qiagen (Valencia, CA, USA). The relative expression of miRNA was calculated by using the comparative $\Delta\Delta C_T$ method, also known as the $2^{-\Delta\Delta CT}$ method.

Laser capture microdissection (LCM) and RNA isolation

Brains of the PITX3/H2BjGFP transgenic mouse, in which the GFP is expressed in the nucleus of midbrain DA neurons, were quickly dissected out and sectioned at 16 μM thickness by cryostat. The midbrain coronal sections (from Bregma −2.92 mm to −3.88 mm) were collected consecutively onto a PAN membrane frame slide (Applied Biosystems) and stored at −80°C until the performance of LCM. The GFP-positive cells in the midbrain were isolated and captured by an ArturusXT microdissection system with fluorescent illumination (Applied Biosystems) at the following working parameters: spot size = 7 μm; power = 50–70 mW and duration = 20 μs. After the GFP-positive neurons from the midbrain were isolated and captured onto LCM Macro Caps (Applied Biosystems), the total RNA was extracted using the PicoPure Isolation kit (Applied biosystems) following the protocol provided by the company.

Immunostaining and light microscopy

As described previously (36), mice were perfused via cardiac infusion with 4% paraformaldehyde in cold phosphate buffered saline (PBS). To obtain frozen sections, brain tissues were removed and submerged in 30% sucrose for 24 h and sectioned at 40 μm thickness with cryostat (Leica CM1950). For immunohistochemistry of human brain sections, paraffin was removed with xylene and the sections were rehydrated in graded ethanol solution. The sections were then processed by microwave to elicit heat-induced antigen retrieval (three times, 5 min at 350 W) in citrate buffer. The procedures for immunostaining were performed as described previously (11). For immunocytochemistry assay, cells were plated on to BD BioCoat poly-D-lysine/laminin cell ware 12 mm round coverslips. For endogenous LRRK2, the cells were fixed with cold methanol for 5 min on ice, and incubated with 10% normal goat serum (Sigma-Aldrich) for 1 h at room temperature to block nonspecific staining. After washing with PBS, the cells were incubated with primary antibody (OC83A; 1:250) for 3 h at room temperature. Alexa 488- or Alexa 568-conjugated secondary antibodies (Invitrogen) were used to visualize the signals. The fluorescent images were captured using a laser scanning confocal microscope (LSM 510; Zeiss, Thornwood, NJ, USA). Paired images were collected at the same gain and offset settings.

Cell line and primary neuron culture

The human embryonic kidney cell line HEK293T and HeLa cells were maintained in Dulbecco's modified Eagle's medium (DMEM-high glucose) containing 10% fetal bovine serum (FBS) in a 5% CO_2 incubator at 37°C. The human neuroblastoma cell line M17 was maintained in Opti-MEM medium (GIBCO BRL) with 10% FBS. Mouse primary neuron cultures were prepared from the cortex of newborn (postnatal day 0) pups, as described previously (36). Briefly, tissues were dissociated with papain (Worthington) buffer, and the cells were plated in poly-D-lysine-coated wells in basal eagle medium (Sigma) containing B27, N2, 1 μM L-glutamine and penicillin/streptomycin (all from Invitrogen). The medium was changed every 2 days.

Constructs and transfection

The pEZX-MR01-miR205 and the miRNA scrambled control clone for pEZX-MR01 were purchased from GeneCopoeia (Germantown, MD, USA). The Cy3-labeled negative control oligonucleotides, negative control oligonucleotides, negative control inhibitor, pre-miR-205, anti-miR-205 inhibitor, pre-miR-29 and miR-29 inhibitor were purchased from Ambion (Austin, TX, USA). Small interfering RNA (siRNA) against human LRRK2 and non-targeting control siRNA

were purchased from Santa Cruz Biotechnology. Lipofectamine 2000 (Invitrogen) or FuGENE HD (Roche Applied Science) was used for the transfection of cell lines, and the calcium phosphate method was used to transfect primary neuron cultures as described previously (37). Briefly, primary neurons cultured for 10 days were transfected with DNA constructs or with a pre miRNA precursor. The DNA–calcium phosphate precipitate was incubated with neuronal cultures for ~ 3 h and then the precipitate was dissolved by incubation in the medium pre-equilibrated in a 10% CO_2 incubator for 20 min in a 5% CO_2 incubator. The efficiency of pre-miRNA oligo transfection was determined using Cy3-labeled pre-miRNA. On average, we achieved 99% efficiency in cells and 60–70% efficiency in neurons. The cells were used 24–48 h after transfection for western blot analysis or immunostaining.

Luciferase activity assays

The 3′-UTR of human *LRRK2* that contains the miR-205 targeting site (5′-AAATAGCTCGTGTGTATGAAGGA-3′) was subcloned into the pGL3 vector (Promega, Madison, WS, USA). The plasmid LRRK2-mUTR containing mutations of the miR-205 target site (5′-AAATAGCTGCTGTGTAGGAAGTA-3′) were also generated. The resulting pGL3-*LRRK2* expression construct was co-transfected with pre-miRNA and pRL-TK vector into the HEK293T cells. Luciferase activity was measured using the dual luciferase assay kit (Promega) and normalized to renila luciferase activity.

Image quantification

To quantify bands detected by western blotting, images were analyzed using Multi Gauge® (ver. 3.0, Fujifilm). For the quantitative assessment of various marker protein accumulations and distributions in the soma or nucleus, images were taken using identical settings and exported to ImageJ (NIH) for imaging analyses. Images were converted to an 8-bit color scale (fluorescence intensity from 0 to 255) using ImageJ. The areas of interest were first selected by Polygon or Freehand selection tools, and then subjected to measurement by mean optical intensities or area fractions. The mean intensity of the background area was subtracted from the selected area to determine the net mean intensity. The length of neurites was also measured using NIH ImageJ as described previously (26). In each case, the bar graphs represent the neurite length or number of 50–100 neurons sampled from three randomly selected microscopic fields of at least two independent experiments from a person blind to the genotype of the neurons.

Statistical analysis

Data from three or more independent experiments are presented as the mean ± standard error of the mean (SEM). Statistical significance was determined using Student's *t*-test followed by a Mann–Whitney test, Tukey–Kramer multiple comparison test or nonparametric Pearson's correlation test. Calculations were performed using GraphPad Prism software.

SUPPLEMENTARY MATERIAL

Supplementary Material is available at *HMG* online.

Conflict of Interest statement. None declared.

FUNDING

This work was supported in part by the Intramural Research Program of the National Institute on Aging at the National Institutes of Health (H.C., AG000944-01), NIH extramural research grants (Y.S., NIHRO1025888 and NIHR01AG032441), and the Research Foundation - Flanders (FWO, grant G.0666.09 to J.-M.T./V.B. and senior researcher fellowship to J.-M.T.), Agency for Innovation by Science and Technology Grant (J.-M.T./V.B., IWT SBO/80020), Katholieke Universiteit Leuven Grants (J.-M.T./V.B, IOF-KP/07/001 and OT/08/052A). Support from the Michael J. Fox Foundation (J.-M.T./V.B.) and the Fund DruwÕ-Eerdekens managed by the King Baudouin Foundation (J.-M.T.) is gratefully acknowledged. We are grateful to the Banner Sun Health Research Institute Brain Donation Program of Sun City, Arizona for the provision of human brain tissue. The Banner Sun Health Research Institute Brain and Body Donation Program and the Arizona Parkinson's Disease Consortium is supported by the National Institute on Aging (P30 AG19610 Arizona Alzheimer's Disease Core Center), the Arizona Department of Health Services (contract 211002, Arizona Alzheimer's Research Center), the Arizona Biomedical Research Commission (contracts 4001, 0011, 05-901 and 1001) and the Michael J. Fox Foundation for Parkinson's Research. We thank Dr Charles H. Adler (Mayo Clinic, Scottsdale, AZ, USA) for critical reading and editing this manuscript. We thank other members of the Cai laboratory for all their support and help.

REFERENCES

1. Schapira, A.H. (1997) Pathogenesis of Parkinson's disease. *Baillieres. Clin. Neurol.*, **6**, 15–36.
2. Ferrer, I., Martinez, A., Blanco, R., Dalfo, E. and Carmona, M. (2011) Neuropathology of sporadic Parkinson disease before the appearance of parkinsonism: preclinical Parkinson disease. *J. Neural. Transm.*, **118**, 821–839.
3. Lanoue, A.C., Dumitriu, A., Myers, R.H. and Soghomonian, J.J. (2010) Decreased glutamic acid decarboxylase mRNA expression in prefrontal cortex in Parkinson's disease. *Exp. Neurol.*, **226**, 207–217.
4. Beach, T.G., Adler, C.H., Lue, L., Sue, L.I., Bachalakuri, J., Henry-Watson, J., Sasse, J., Boyer, S., Shirohi, S., Brooks, R. *et al.* (2009) Unified staging system for Lewy body disorders: correlation with nigrostriatal degeneration, cognitive impairment and motor dysfunction. *Acta. Neuropathologica.*, **117**, 613–634.
5. Dumitriu, A., latourelle, J.C., Hadzi, T.C., Pankratz, N., Garza, D., Miller, J.P., Vance, J.M., Foroud, T., Beach, T.G. and Myers, R.H. (2012) Gene expression profiles in Parkinson disease prefortal cortex implicate FOXO1 and gene under its transcriptional regulation. *PLoS Genet.*, **8**, e1002794.
6. Hardy, J., Cai, H., Cookson, M.R., Gwinn-Hardy, K. and Singleton, A. (2006) Genetics of Parkinson's disease and parkinsonism. *Ann. Neurol.*, **60**, 389–398.
7. Paisan-Ruiz, C., Jain, S., Evans, E.W., Gilks, W.P., Simon, J., van der, B.M., Lopez, D.M., Aparicio, S., Gil, A.M., Khan, N. *et al.* (2004) Cloning of the gene containing mutations that cause PARK8-linked Parkinson's disease. *Neuron*, **44**, 595–600.
8. Zimprich, A., Biskup, S., Leitner, P., Lichtner, P., Farrer, M., Lincoln, S., Kachergus, J., Hulihan, M., Uitti, R.J., Calne, D.B. *et al.* (2004) Mutations

in LRRK2 cause autosomal-dominant Parkinsonism with pleomorphic pathology. *Neuron*, **44**, 601–607.
9. Satake, W., Nakabayashi, Y., Mizuta, I., Hirota, Y., Ito, C., Kubo, M., Kawaguchi, T., Tsunoda, T., Watanabe, M., Takeda, A. *et al.* (2009) Genome-wide association study identifies common variants at four loci as genetic risk factors for Parkinson's disease. *Nat. Genet.*, **41**, 1303–1307.
10. Simon-Sanchez, J., Schulte, C., Bras, J.M., Sharma, M., Gibbs, J.R., Berg, D., Paisan-Ruiz, C., Lichtner, P., Scholz, S.W., Hernandez, D.G. *et al.* (2009) Genome-wide association study reveals genetic risk underlying Parkinson's disease. *Nat. Genet.*, **41**, 1308–1312.
11. Lin, X., Parisiadou, L., Gu, X.L., Wang, L., Shim, H., Sun, L., Xie, C., Long, C.X., Yang, W.J., Ding, J. *et al.* (2009) Leucine-rich repeat kinase 2 regulates the progression of neuropathology induced by Parkinson's-disease-related mutant alpha-synuclein. *Neuron*, **64**, 807–827.
12. Bartel, D.P. (2004) MicroRNAs: genomics, biogenesis, mechanism, and function. *Cell*, **116**, 281–297.
13. Kosik, K.S. (2006) The neuronal microRNA system. *Nat. Rev. Neurosci.*, **7**, 911–920.
14. Hebert, S.S. and De Strooper, B. (2009) Alterations of the microRNA network cause neurodegenerative disease. *Trends Neurosci.*, **32**, 199–206.
15. Kim, J., Inoue, K., Ishii, J., Vanti, W.B., Voronov, S.V., Murchison, E., Hannon, G. and Abeliovich, A. (2007) A MicroRNA feedback circuit in midbrain dopamine neurons. *Science*, **317**, 1220–1224.
16. Junn, E., Lee, K.W., Jeong, B.S., Chan, T.W., Im, J.Y. and Mouradian, M.M. (2009) Repression of alpha-synuclein expression and toxicity by microRNA-7. *Proc. Natl Acad. Sci. USA*, **106**, 13052–13057.
17. Gehrke, S., Imai, Y., Sokol, N. and Lu, B. (2010) Pathogenic LRRK2 negatively regulates microRNA-mediated translational repression. *Nature*, **466**, 637–641.
18. Arlotta, P., Molyneaux, B.J., Jabaudon, D., Yoshida, Y. and Macklis, J.D. (2008) Ctip2 controls the differentiation of medium spiny neurons and the establishment of the cellular architecture of the striatum. *J. Neurosci.*, **28**, 622–632.
19. Bartel, D.P. (2009) MicroRNAs: target recognition and regulatory functions. *Cell*, **136**, 215–233.
20. Lewis, B.P., Shih, I.H., Jones-Rhoades, M.W., Bartel, D.P. and Burge, C.B. (2003) Prediction of mammalian microRNA targets. *Cell*, **115**, 787–798.
21. Lewis, B.P., Burge, C.B. and Bartel, D.P. (2005) Conserved seed pairing, often flanked by adenosines, indicates that thousands of human genes are microRNA targets. *Cell*, **120**, 15–20.
22. Fletcher, A.M., Heaford, A.C. and Trask, D.K. (2008) Detection of metastatic head and neck squamous cell carcinoma using the relative expression of tissue-specific mir-205. *Transl. Oncol.*, **1**, 202–208.
23. Wu, H. and Mo, Y.Y. (2009) Targeting miR-205 in breast cancer. *Expert Opin. Ther. Targets*, **13**, 1439–1448.
24. Chendrimada, T.P., Gregory, R.I., Kumaraswamy, E., Norman, J., Cooch, N., Nishikura, K. and Shiekhattar, R. (2005) TRBP recruits the dicer complex to Ago2 for microRNA processing and gene silencing. *Nature*, **436**, 740–744.
25. Cheng, A.M., Byrom, M.W., Shelton, J. and Ford, L.P. (2005) Antisense inhibition of human miRNAs and indications for an involvement of miRNA in cell growth and apoptosis. *Nucleic Acids Res.*, **33**, 1290–1297.
26. Parisiadou, L., Xie, C., Cho, H.J., Lin, X., Gu, X.L., Long, C.X., Lobbestael, E., Baekelandt, V., Taymans, J.M., Sun, L. *et al.* (2009) Phosphorylation of ezrin/radixin/moesin proteins by LRRK2 promotes the rearrangement of actin cytoskeleton in neuronal morphogenesis. *J. Neurosci.*, **29**, 13971–13980.
27. Li, Y., Liu, W., Oo, T.F., Wang, L., Tang, Y., Jackson-Lewis, V., Zhou, C., Geghman, K., Bogdanov, M., Przedborski, S. *et al.* (2009) Mutant LRRK2(R1441G) BAC transgenic mice recapitulate cardinal features of Parkinson's disease. *Nat. Neurosci.*, **12**, 826–828.
28. Galter, D., Westerlund, M., Carmine, A., Lindqvist, E., Sydow, O. and Olson, L. (2006) LRRK2 expression linked to dopamine-innervated areas. *Ann. Neurol.*, **59**, 714–719.
29. Giasson, B.I. and Van Deerlin, V.M. (2008) Mutations in LRRK2 as a cause of Parkinson's disease. *Neurosignals*, **16**, 99–105.
30. Sharma, S., Bandopadhyay, R., Lashley, T., Renton, A.E., Kingsbury, A.E., Kumaran, R., Kallis, C., Vilarino-Guell, C., O'Sullivan, S.S., Lees, A.J. *et al.* (2011) LRRK2 expression in idiopathic and G2019S positive Parkinson's disease subjects: A morphological and quantitative study. *Neuropathol. Appl. Neurobiol.*, **37**, 777–790.
31. Devine, M.J., Kaganovich, A., Ryten, M., Mamais, A., Trabzuni, D., Manzoni, C., McGoldrick, P., Chan, D., Dillman, A., Zerle, J. *et al.* (2011) Pathogenic LRRK2 mutations do not alter gene expression in cell model systems or human brain tissue. *PLoS ONE*, **6**, e22489.
32. Beach, T.G., Sue, L.I., Walker, D.G., Roher, A.E., Lue, L., Vedders, L., Connor, D.J., Sabbagh, M.N. and Rogers, J. (2008) The Sun Health Research Institute Brain Donation Program: description and experience, 1987–2007. *Cell Tissue Bank*, **9**, 229–245.
33. Taymans, J.M., Van den, H.C. and Baekelandt, V. (2006) Distribution of PINK1 and LRRK2 in rat and mouse brain. *J. Neurochem.*, **98**, 951–961.
34. Song, H. and Bu, G. (2009) MicroRNA-205 inhibits tumor cell migration through down-regulating the expression of the LDL receptor-related protein 1. *Biochem. Biophys. Res. Commun.*, **388**, 400–405.
35. Bhatnagar, N., Li, X., Padi, S.K., Zhang, Q., Tang, M.S. and Guo, B. (2010) Downregulation of miR-205 and miR-31 confers resistance to chemotherapy-induced apoptosis in prostate cancer cells. *Cell Death Dis.*, **1**, e105.
36. Cai, H., Lin, X., Xie, C., Laird, F.M., Lai, C., Wen, H., Chiang, H.C., Shim, H., Farah, M.H., Hoke, A. *et al.* (2005) Loss of ALS2 function is insufficient to trigger motor neuron degeneration in knock-out mice but predisposes neurons to oxidative stress. *J. Neurosci.*, **25**, 7567–7574.
37. Lai, C., Xie, C., McCormack, S.G., Chiang, H.C., Michalak, M.K., Lin, X., Chandran, J., Shim, H., Shimoji, M., Cookson, M.R. *et al.* (2006) Amyotrophic lateral sclerosis 2-deficiency leads to neuronal degeneration in amyotrophic lateral sclerosis through altered AMPA receptor trafficking. *J. Neurosci.*, **26**, 11798–11806.
38. Garcia, D.M., Baek, D., Shin, C., Bell, G.W., Grimson, A. and Bartel, D.P. (2011) Weak seed-pairing stability and high target-site abundance decrease the proficiency of lsy-6 and other miRNAs. *Nat. Struct. Mol. Biol.*, **18**, 1139–1146.